

Final Draft
of the original manuscript:

Obasi, C.G.; Ferry, O.M.; Ebel, T.; Bormann, R.:

**Influence of processing parameters on mechanical properties of
Ti-6Al-4V alloy fabricated by MIM**

In: Materials Science and Engineering A (2010) Elsevier

DOI: 10.1016/j.msea.2010.02.070



Influence of processing parameters on mechanical properties of Ti-6Al-4V alloy fabricated by MIM



G. C. Obasi, O.M. Ferri, T. Ebel, R. Bormann

GKSS Research Centre, Institute of Materials Research, Max-Planck-Straße 1,

D-21502 Geesthacht, Germany.



Keywords: Metal Injection Molding; Debinding parameters; Sintering parameters; Mechanical properties

Abstract

This study presents the results of systematic variation of essential processing parameters with regard to thermal debinding and sintering of components fabricated by MIM using Ti-6Al-4V powder. The investigation aims at the understanding of the particular influence these parameters have on the mechanical properties of the sintered parts. This study shows that the debinding parameters appear to be rather uncritical, whereas sintering and cooling rates as well as maximum temperature are important in terms of their effect on tensile strength. Contrary to the strength, the ductility remains nearly unaffected. Based on these results, samples displaying a yield strength of 757 MPa, UTS of 861 MPa and a plastic elongation of more than 14% were produced. These values meet the requirements of the ASTM B 348-02 for titanium alloy grade 23.

1 Introduction

The excellent properties of Ti-6Al-4V alloy such as high specific strength, high corrosion resistance in many media, and excellent biocompatibility have attracted attention for the last decades and make this alloy an excellent choice for many applications, including medical implants, automotive components, and air craft parts [1]. However, the utilisation of this alloy has been limited due to the high costs related to the raw material, the multi-step fabrication process, and associated geometry design constraints. Metal Injection Moulding (MIM) is a manufacturing process candidate that can be applied in order to overcome some of these drawbacks.

MIM offers a net-shape or near net-shape fabrication route for making complex shaped parts in large volumes. In the past few years, the development of this process has been successful. The

problem of contamination with oxygen, nitrogen and carbon during debinding and sintering operations, which strongly influences the mechanical properties, can largely be overcome. Parts based on Ti-6Al-4V with reasonable strength-levels and large plastic elongations can be achieved today (e.g. [2-4]). However, with respect to further optimization, the effect of microstructural features such as final porosity, size of the lamellar colonies, and interstitial element content on the mechanical properties of Ti-6Al-4V alloy components fabricated by MIM is not totally understood.

In this study, the MIM process was used to produce samples using Ti-6Al-4V alloy powder (<45 μ m). Sintering and debinding conditions were varied in order to analyse the effect on the mechanical and microstructural properties of the components.

2 Sample preparation

The samples were prepared by a Metal Injection Moulding process as described in [5] using a wax and polymer based feedstock. Ti-6Al-4V ELI (ASTM grade 23) gas atomised powder of spherical shape with a particle diameter smaller than 45 μ m was used in this study. The chemical composition of the powder according to the supplier is given in Table 1.

The binder system used was a mixture of 35 wt. % polymer, 5 wt. % stearic acid and 60 wt% paraffin wax. The feedstock used in the experiments had a binder system fraction of 8.5 wt. %, except during the investigation of the influence of sintering time, where a feedstock with 10 wt. % binder was used. The metal powder and the binder system were mixed in a Z-blade mixer under argon atmosphere. After granulation, the feedstock was injection molded into a standard “dog bone” shape tensile specimens, with a nominal length of about 89 mm and thickness of 5 mm.

The paraffin wax was removed by chemical debinding with heptane at 40 °C for 20 h. The thermal debinding of the polymer component and the sintering of the powder were performed in a cold-wall furnace with tungsten heating elements and molybdenum shield packs. The thermal debinding process was conducted under argon atmosphere followed by sintering under high vacuum ($\sim 10^{-4}$ mbar).

After sintering, the levels of oxygen, carbon and nitrogen were determined using a conventional LECO melt extraction system.

The apparent density of the sintered parts was measured by the immersion method outlined in ASTM B311.

Optical microscopy (Olympus PMG3) and Scanning Electron Microscopy (ZEISS-DSM962) were used in order to investigate the sintered microstructure and the tensile fracture surface, respectively. An imaging analysis system was applied for the estimation of the average lamellar colony size and alpha lamellae width.

The tensile tests were carried out on a servo-hydraulic structural test machine equipped with a 100 kN load cell at room temperature. A strain rate of $3.5 \times 10^{-5} \text{ s}^{-1}$ was applied.



3 Results and Discussion

The heating rate to debinding temperature dT_{debind} , the heating rate to sintering temperature dT_{sinter} , the sintering temperature, the sintering time, and the cooling rate were identified as essential parameters, which could influence the mechanical properties of the sintered part. All parameters could potentially change the content of interstitials, the final density, grain size or grain structure. In the following sections, the results from the variation of these parameters with respect to mechanical and microstructural properties are reported.

All samples described in the following sections were analysed with respect to their content of interstitial elements O, N and C, because of the influence of these interstitial impurities on strength and ductility. However, the deviation in these contents during variation of the sintering

parameters was not significant. The analysed average values were 2154 ± 91 $\mu\text{g/g}$ oxygen, 378 ± 26 $\mu\text{g/g}$ carbon and 182 ± 31 $\mu\text{g/g}$ nitrogen.

No dependence of these values on the varied processing parameters could be detected. Therefore, the pick up of interstitials during processing was considered to be constant within this investigation and was not taken into account in the following discussion.

3.1 Variation of sintering temperature

Table 2 shows the influence of maximum sintering temperature on the tensile properties and the microstructure of the sintered samples. The yield strength and the UTS increase significantly as sintering temperature increases; however, no clear effect of the maximum sintering temperature on the plastic elongation was observed.

Fig 1 (a and b) shows the optical micrographs of two samples sintered at 1250 °C and 1400 °C. They reveal a typical fully lamellar microstructure with the additional presence of pores.

As expected, the observed higher strength for samples sintered at higher temperature can be related to differences in the microstructural features. The level of densification (amount of pores) seems to be the most relevant parameter that influenced the tensile strength. This result is in line with previous works [2-4] where samples with lower porosity exhibited higher yield strength and UTS.

Diametrical to the positive effect of the lower porosity on strength should be the coarsening of colony size observed for samples sintered at higher temperatures (Table 2). This significant coarsening effect was already investigated by Itoh et al. [3] and Zhang et al. [4], and this effect is related to the predominant influence of the coarsening mechanism over densification during sintering at high temperatures. However, with respect to tensile strength, the positive effect of the higher density overcomes the negative effect of the coarser grains. On the other hand, for components exposed to fatigue load, the coarser structure could be detrimental. Therefore, in order to compromise densification and microstructure size, the maximum sintering temperature used for the following experiments was 1350 °C.

3.2 Variation of heating rate to sintering temperature dT_{sinter}

The heating rate dT_{sinter} describes the temperature change per minute during heating from debinding to maximum sintering temperature. Table 3 shows the measured properties of samples sintered at the same maximum sintering temperature (1350 °C), but with different heating rates.

As indicated in Table 3, applying a heating rate dT_{sinter} of 15 °C/min promotes a certain deterioration of the tensile properties. This is especially true in terms of plastic elongation. Such behaviour is not fully understood yet, but it is possible to assume that at a heating rate of 15 °C/min, the coarsening process overcomes the densification process faster than it does at slower heating rate. This assumption is in agreement with the final densification results presented in Table 3. On the other hand, it is important to note that this degradation of the tensile properties was not observed for the samples sintered at heating rates of 10 °C/min and 5 °C/min, even though the densification was smaller than it was for the samples with a higher heating rate dT_{sinter} . This is an indication of a maximum rate existing above 10 °C/min which should not be exceeded to avoid embrittlement.

3.3 Variation of sintering time

The effect of changing the sintering time at the isotherm of 1350 °C was investigated on samples with a binder content of 10 wt. %. The comparison with samples with 8.5 wt. % binder content exposed to the same process revealed a lower density of the 10 wt. % samples, probably due to a slightly larger distance between the particles prior to sintering. This lower density led to a lower strength of the sintered parts, whereas the ductility was not affected.

As expected, sintering for only one instead of two hours reduced the strength significantly as seen in Table 4. Again, the reason for this is assumed to be the lower densification. On the other hand, the ductility is left unaffected.

Applying a prolonged sintering time of 10 hours increased densification and strength significantly. No additional oxygen pickup was observed. However, due to the long processing time, the colony size became much larger, which might influence the fatigue properties unfavourably. The importance of a fine microstructure for good fatigue behaviour of MIM processed components made from Ti-6Al-4V powder is discussed in [6].

Tensile fractography


The Ti-6Al-4V alloy specimens fracture surfaces are shown in Fig 2 (a, b, c and d). A clear difference in fracture surface behaviour amongst the different sintering parameters is observed. The specimens sintered at lower temperatures (Fig. 2a) and the specimens with a heating rate dT_{sinter} of 15 °C/min (Fig. 2b) exhibit big cavities apart from the existing pores and few dimples on the tensile fracture surface. This behaviour can be an indication of a mixed fracture mechanism (transgranular and intergranular). The sample may have fractured intergranularly in some areas where the connections between the grains were not well established due to an incomplete sintering process, and in other areas, the samples presented a typical ductile fracture surface with fine dimples (white arrows indicate the fine dimples on the tensile fracture surface). The presence of finely dimpled structure on the tensile fracture surface was much more pronounced for samples sintered at 1350 °C with a heating rate dT_{sinter} of 5°C/min (Fig. 2c). A possible explanation for such behaviour can be related to the sintering process. As described by German [7], the two main mechanisms of densification and coarsening describe the sintering behaviour of a specific material. For most materials, during the final sintering process (usually at relatively high temperatures), the coarsening effect overcomes the densification effect mainly due to a phenomenon called “breakaway”. Breakaway is the isolation of the pores into grain interiors. This occurs due to the fact that beyond certain point the driving force for grain growth exceeds the pore restraining force.

Therefore, at a higher heating rate dT_{sinter} , one can expect that the coarsening mechanism will be activated earlier than at a lower heating rate as discussed above. The results of grain size and densification for the samples sintered with heating rates of 5 and 15 °C/min illustrated in Table 3 support to this assumption. In fact, it should be noted that the lower presence of fine dimples on the tensile fracture surface of samples sintered at lower temperatures or with higher heating rate is an indication of a sintering process that is not optimal.

Fig. 2d shows the fracture surface of a sample with 10 wt. % binder content sintered for 10 hours. It is entirely covered by fine dimples and corresponds very well with the fracture surface sample with 8.5 wt. % binder that was sintered for two hours, shown in Fig. 2c. In summary, the amount and structure of dimples appears to correspond with the strength of the samples, as indicated in Tables 3 and 4. However, it is important to note that it was not possible to relate the amount of dimples to the final plastic elongation, since samples sintered at 1250 °C exhibited almost no dimples, but still showed a plastic elongation in the range of samples sintered at 1350 °C which had a high amount of fine dimples. As of yet, it is not possible to totally understand, on

micromechanical level, the influence of pores and maximum sintering temperature on the ductility, especially when the samples exhibit a relatively low fraction of remaining pores.

3.4 Variation of cooling rate

The variation of the cooling rate after sintering is presented in Table 5. A significant, but unsystematic influence on the tensile properties of the sintered part was observed. While the samples cooled at a rate of 20 °C/min reveal approximately the same tensile strength as but a higher ductility than the reference samples cooled at a rate of 10 °C/min, a small but significant improvement of the tensile strength was observed by applying a slower cooling rate of 5 °C/min. The strength is increased by about 10 MPa and the plastic elongation by about 2%. It can be assumed that the improved ductility is mainly due to the lower porosity, which was connected to the longer over-all time the sample is exposed to high temperature. 

On the other hand, the highest strength was accomplished by using a cooling rate of 66 °C/min, which corresponds to a simple switch off of the furnace used. The rate was calculated from the time of uncontrolled cooling from 1350 °C to 1000 °C. Although the densification was relatively low, the observed improvement in strength was expected due to the decrease in α lamellae width as given in Table 5. It has been reported by Filip et al. [8] and Lütjering [9] that the mechanical properties strongly depend on the applied cooling rate since microstructural features such as α lamellae colony width, α colony size, and β grain size are affected. Fig. 3 shows micrographs of the lamellae for the samples cooled with 10 °C / min and 66 °C / min.

3.4 Variation of heating rate to debinding temperature dT_{debind}

The heating rate dT_{debind} denotes the temperature change per minute from room temperature to the debinding isotherm, in this study fixed at 450 °C. The thermal debinding process can influence the mechanical properties on two ways. Firstly, during decomposition of the polymer, carbon can diffuse into the alloy powder as an interstitial element, and secondly, accelerated debinding can destroy the structure of the part by pressure build-up. Therefore, a possible effect of the heating rate dT_{debind} on the mechanical properties was investigated.

Table 6 shows the test results of the samples debound at different heating rates and sintered at 1350 °C. The table indicates similar tensile properties and identical densification of all parts.

As illustrated in Table 6, there was no significant change in the carbon content of the compacts. This indicates that the binder was completely removed at all investigated heating rates. Furthermore, even the samples debound with a higher heating rate dT_{debind} did not show any surface defects. This result agrees with previous investigation of Yimin et al. [10], who reported that increasing the heating rate did not promote defects in compacts with thicknesses smaller than 10 mm. One has to keep in mind, though, that the optimal heating rate depends on the geometry of the particular component. Nevertheless, it can be concluded from this study that there is a rather wide scope within which this parameter can be varied without influencing the properties of the sintered part.

4 Summary and conclusion

The essential process parameters for thermal debinding and sintering within the MIM processing of Ti-6Al-4V were varied in order to investigate their specific influence on the mechanical properties of the sintered parts. The study was aimed at both optimising the mechanical properties and obtaining better knowledge that can be directed towards process controlling during production.

A clear dependence of the tensile strength on the sintering temperature and time due to differences in densification was observed, while the interstitial content remained constant. On the other hand, the microstructure became coarser because of sintering at higher temperatures or longer times, which might deteriorate the fatigue behaviour. Therefore it is recommended to choose a sintering temperature and time in dependence of the type of loading the component will be exposed to. As a compromise, a sintering temperature of 1350 °C seems to be appropriate for most applications.

Within the range of 2.0 % to 5.4 % residual porosity observed in this study, no clear influence of the density on ductility was detected.

The heating rate to debinding temperature dT_{debind} can be varied within a rather large range without affecting the properties of the sintered parts. This indicates that this parameter is not critical and should be adjusted, aiming for short processing times.

Contrary to dT_{debind} , the subsequent heating rate dT_{sinter} up to the sintering temperature appears to be critical and influences final density and grain size. A 10 °C/min heating rate should not be exceeded for the powder used in this study.

Fast cooling is beneficial with respect to mechanical properties due to the establishment of fine α lamellae. Simultaneously, a favourable shorter processing time can be achieved.

Taking into account all these factors, tensile properties of $\sigma_{0.2} = 757$ MPa, UTS = 861 MPa and $\varepsilon = 14.3$ % were achieved in this study. These mechanical properties meet the requirements of the ASTM B 348-02 for grade 23. Furthermore, it is important to note that Zhang et al. [4] obtained an even higher tensile strength, but this was achieved not without detriment to plastic elongation. However, in this investigation, the increase of tensile strength was accompanied by retained excellent ductility. Such a result was possible due to the fact that the pick up of interstitial elements during the sintering process was relatively low and constant.



6 References:

- [1] F.H. Froes, J. Lombardi, L.Lavoie, J. Fravel, M. Godfrey, Titanium Powder Injection Molding – A Cost Effective Alternative, in: TMS Symposium on High Performance Metallic Materials for Cost Sensitive, TMS, Washington, 2002.
- [2] B. Oger, T. Ebel, W. Limberg, The manufacture of highly-ductile and geometrically complex MIM-parts based on TiAl6V4, in: EUROPM 2006, vol 2, EPMA, 2006, pp. 191-196.
- [3] Y. Itoh, T. Harikou, K. Sato, H. Miura, Improvement of ductility for injection moulding Ti-6Al-4V alloy, in: EUROPM2004, vol 4, EPMA, 2004.
- [4] R. Zhang, J. Kruszewski, J. Lo, Powder injection moulding international 2 (2008) 74-78.
- [5] E. Aust, W. Limberg, R. Gerling, B. Oger, T. Ebel, Advanced Engineering Materials 8 (2006) 365-370.
- [6] O.M. Ferri, T. Ebel, R. Bormann, Mater. Sci. Eng. A 504 (2009) 107-113.
- [7] R. M. German, Powder Metallurgy Science, MPIF, Princeton, 1984.

[8] R. Filip, W. Z. K. Kubiak, J. Sieniawski, *Journal of Materials Processing Technology* 2003 (2003) 84-89.

[9] G. Lütjering, *Mater. Sci. Eng. A* 243 (1998) 32-45.

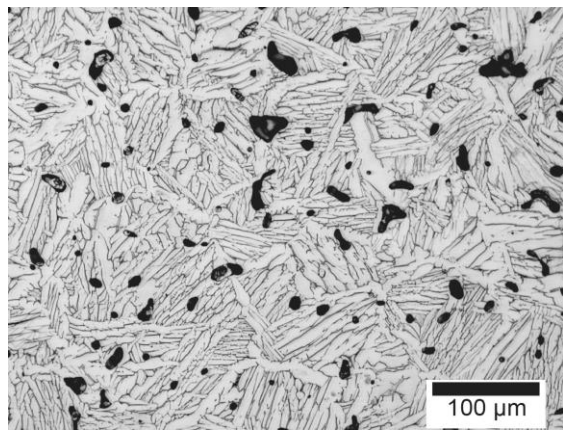
[10] L. Yimin, F. Jiang, L. Zhao, B. Huang, *Mater. Sci. Eng. A* 362 (2003) 292-299.



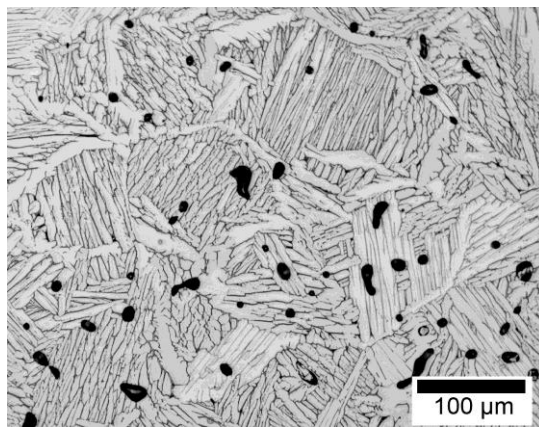
Acknowledgement

This project has been supported by European Commission –Education and Training and GKSS Research Centre, Germany.

.



(a)



(b)

Fig. 1 Optical micrographs of samples sintered at different temperatures (a) at 1250 °C (b) at 1400 °C, revealing different colony size.

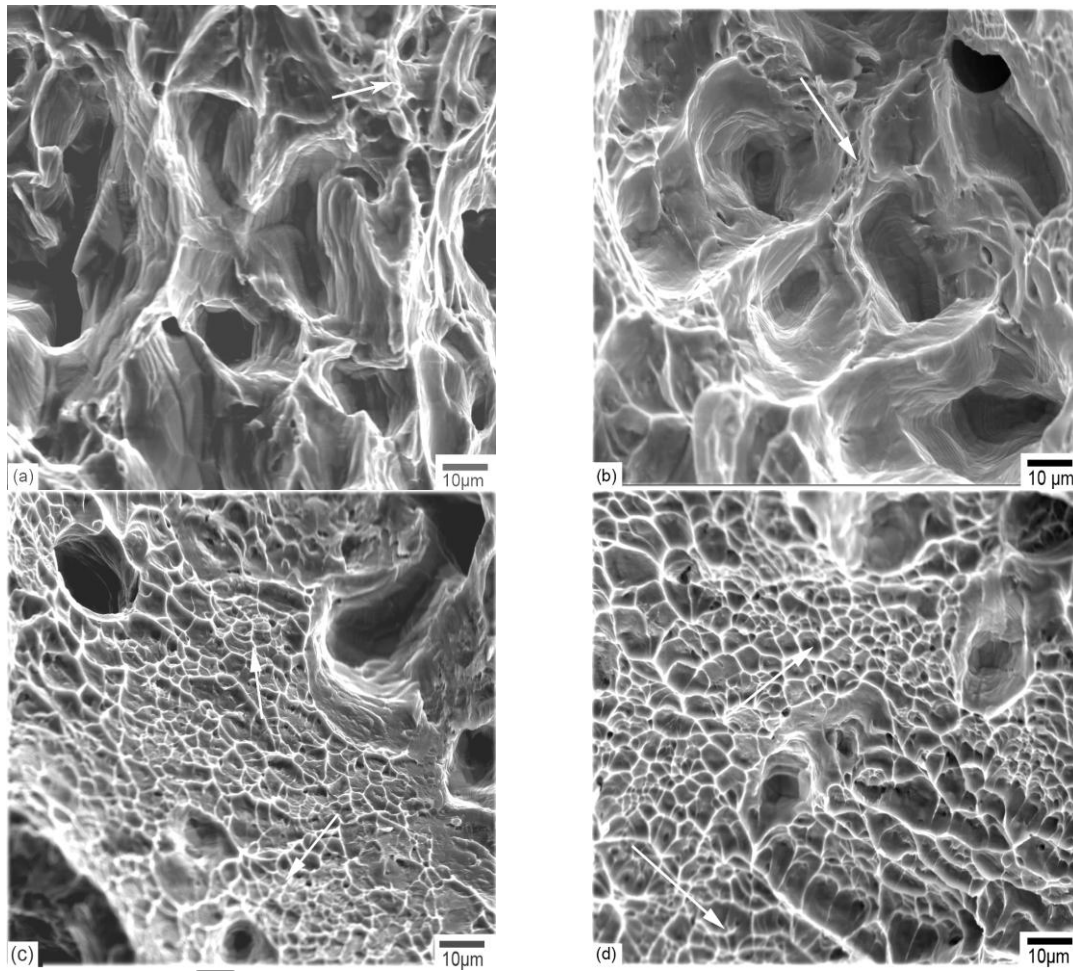
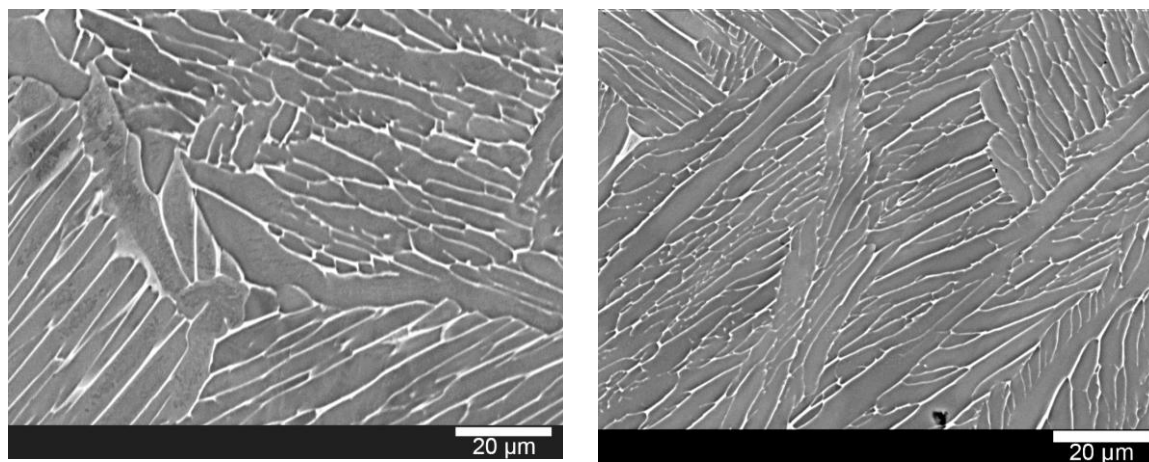


Fig. 2 SEM in **BS** mode micrographs of the fracture surfaces of samples sintered (a) at 1250 °C (b) at 1350 °C with heating rate dT_{sinter} of 15 °C/min, (c) at 1350 °C with heating rate dT_{sinter} of 5 °C/min and (d) at 1350 °C sintered for 10 h (10% binder content).



(a)

(b)

Fig. 3 Comparison of α lamellae width in two samples cooled with rate of (a) $10\text{ }^\circ\text{C} / \text{min}$ and (b) $66\text{ }^\circ\text{C} / \text{min}$. The white features represents the β -phase, the dark ones the α -phase

Element	Al	V	C	Fe	O	N	H	Ti
Wt %	6.14	4.0	0.020	0.150	0.100	0.010	0.004	Bal.

Table 1 Chemical composition of the powder (wt. %).

Temp.(°C)	Tensile properties			Microstructural features	
	Yield stress (MPa)	UTS (MPa)	Elongation (%)	Average colony size (μm)	Densification (%)
1250	703 \pm 6	806 \pm 3	13.7 \pm 1	92	96.2
1300	720 \pm 4	821 \pm 2	14.0 \pm 2	93	96.4
1350	728 \pm 5	832 \pm 2	13.4 \pm 1	102	97.1
1400	744 \pm 6	846 \pm 5	14.8 \pm 2	120	97.3

Table 2 Variation of sintering temperature.

Heating rate dT_{sinter} ($^{\circ}\text{C}/\text{min}$)	Tensile properties			Microstructural features	
	Yield stress (MPa)	UTS (MPa)	Elongation (%)	Average colony size (μm)	Densification (%)
5	728 \pm 5	832 \pm 2	13.4 \pm 0.5	102	97.1
10	731 \pm 3	832 \pm 3	14.9 \pm 1.7	104	96.8
15	723 \pm 5	825 \pm 3	11.2 \pm 0.4	112	96.6

Table 3 Variation of heating rate. Sintering temperature 1350 $^{\circ}\text{C}$.

Sintering time (hours)	Tensile properties			Microstructural features	
	Yield stress (MPa)	UTS (MPa)	Elongation (MPa)	Average colony size (μm)	Densification (%)
1	699 \pm 5	801 \pm 5	13.9 \pm 0.1	94	94.6
2	720 \pm 2	824 \pm 4	14.3 \pm 0.7	93	95.7
10	753 \pm 1	853 \pm 1	13.0 \pm 0.2	157	98.0

Table 4 Variation of sintering time. Sintering temperature 1350 $^{\circ}\text{C}$, binder content 10 wt.%, heating rate dT_{sinter} of 10 $^{\circ}\text{C}/\text{min}$.

Cooling rate (°C / min)	Tensile properties			Microstructural features		
	Yield stress (MPa)	UTS (MPa)	Elongation (%)	Average colony size (μm)	Densification (%)	α lamellae width (μm)
5	739 \pm 3	842 \pm 2	15.5 \pm 1	113	97.3	14
10	728 \pm 5	832 \pm 2	13.4 \pm 1	102	97.1	14
20	731 \pm 2	835 \pm 1	14.4 \pm 1	92	96.8	10
66	757 \pm 4	861 \pm 4	14.3 \pm 0.4	95	96.8	7

Table 5 Variation of cooling rate. Sintering temperature 1350 °C, heating rate dT_{sinter} 5°C/min.

Heating rate dT_{debind} (°C/min)	Tensile properties			Microstructural features		
	Yield stress (MPa)	UTS (MPa)	Elongation (%)	Average colony size (μm)	Densification (%)	Carbon content ($\mu\text{g/g}$)
2	728 \pm 5	832 \pm 2	13.4 \pm 0.5	91	97.1	400 \pm 34
5	734 \pm 3	835 \pm 2	14.0 \pm 0.4	92	97.1	395 \pm 14
10	728 \pm 3	828 \pm 4	13.5 \pm 1	92	97.1	403 \pm 47

Table 6 Variation of heating rate dT_{debind} . Sintering temperature 1350 °C, heating rate dT_{sinter} 5°C/min.